Hydrogen Atomic and Molecular Emission Locations and Intensities in the LHD Edge Plasma Determined from Simultaneously Observed Polarization Spectra*)

Keisuke FUJII, Keiji SAWADA[1)], Motoshi GOTO[2)], Shigeru MORITA[2)] and Masahiro HASUO

Graduate School of Engineering, Kyoto University, Katsura, Kyoto 615-8540, Japan
[1)]*Department of Applied Physics, Faculty of Engineering, Shinshu University, Nagano 380-8553, Japan*
[2)]*National Institute for Fusion Science, 322-6 Oroshi-cho, Toki 509-5292, Japan*

(Received 25 November 2014 / Accepted 12 March 2015)

We observed polarization-resolved emission spectra of the Balmer-α, -β, and -γ lines of hydrogen atoms and the Q branches of the Fulcher-α band of hydrogen molecules simultaneously with six lines of sight in a poloidal cross section of the Large Helical Device (LHD). From the fit of the spectra including the line splits and their polarization dependence due to the Zeeman effect, we determined the emission locations, intensities and temperatures of the atoms and molecules. The determined emission locations of the hydrogen atoms were just outside the last closed flux surface and the intensities showed small dependence on the location. The emission locations of the molecules were rather around the divertor legs and their emission intensities showed location dependences. The determined atomic temperature was about 1 eV and the molecular rotational temperature was 0.04~0.07 eV, both of which showed no systematic dependence on the location within the experimental accuracy.

Keywords: Polarization spectroscopy, Balmer emission spectra, Fulcher-α emission spectra, Zeeman effect, Emission locations and intensities, LHD edge plasma

DOI: 10.1585/pfr.10.3402041

1. Introduction

In fusion relevant magnetic plasma confinement devices, ionizations of neutral hydrogen atoms and molecules give dominant source of the charged particles. The understandings of their dynamics are demanded for achieving high performance plasmas [1, 2].

In the peripheral regions of the devices, the neutral hydrogen molecules are generated by desorption and/or recombination on divertor plates and some of them travel toward the plasma. Since the electron temperature and density are high enough to ionize or dissociate most of the molecules by electron impacts even in the outside region of the confined plasma, for example in the divertor leg or the ergodic layer. Most of the neutral hydrogen atoms generated by dissociation, desorption, or recombination, are also ionized outside the confined region, while small part of the atoms penetrate deeply inside the core plasma through charge exchange collision with hot protons [3, 4].

Since the molecular and atomic emissions are mainly generated in their ionization locations, such hydrogen dynamics have been observed by the emission measurement [5, 6]. In a passive measurement, the integrated intensity along a line of sight (LOS) is observed, and then no spatial information along the LOS is obtained. Weaver *et al*. have proposed a method to determine the two emission locations of the atomic Balmer-α line along the LOS by comparing its Zeeman split and the spatial distribution of the magnetic field [7]. A multiple LOSs measurement with this technique has been performed by Shikama *et al*. [8]. Iwamae *et al*. have demonstrated the emission location measurement of the hydrogen atoms for the Large Helical Device (LHD) with an aid of the polarization-resolved spectroscopic technique [9, 10].

On the other hand, emission lines of hydrogen molecules in fusion devices have been observed by several groups [11, 12]. Vibrational and rotational temperatures of the molecules have been determined from the intensities of several emission lines in the Fulcher-α band [13, 14]. The Zeeman split of the molecular lines has been also observed [15].

For the purpose of further improving this technique, we recently demonstrated a method to observe several emission spectra of hydrogen atoms and molecules simultaneously with developing a multi-wavelength high-resolution (MH) spectrometer [16, 17]. From the observed Zeeman splits of the atomic and molecular lines, we have shown the difference of the atomic and molecular emission locations in the LHD [18]. In this paper, we describe the multiple LOSs measurement of the atomic and molecular emissions for the investigation of the location and intensity distributions in the LHD.

author's e-mail: fujii@me.kyoto-u.ac.jp

*) This article is based on the presentation at the 24th International Toki Conference (ITC24).

2. Experiment

Figures 1 (a) and (b) show the toroildal and poloidal cross sections of the LHD. In the figures, the last closed flux surface (LCFS) is shown by black solid curves. The closed magnetic flux surfaces are shown by gray curves inside the LCFS. The gray region outside the LCFS indicates the ergodic layer which consists of a large number of open magnetic field lines whose connection length ranges from several ten to several thousand meters. The divertor plates and the first walls are illustrated by black bold lines. The major radius of the plasma axis and magnetic field strength at the axis are 3.6 m and 2.85 T, respectively.

A hydrogen plasma is observed with six LOSs, which are shown by horizontal lines in Fig. 1 (b). For each LOS, we set a polarization-resolved optics (PSO) which consists of a Glan-Thompson prism and two focusing lenses [9]. Two orthogonal linear polarization components of the emission from the plasma are resolved by the PSO. The two polarization components, i.e. ordinary ray (o-ray) and extraordinary ray (e-ray) of the Glan-Thompson prism are introduced into two optical fibers separately. We adjust the angle of each PSO so that the direction of the e-ray is parallel to the magnetic field direction at the inner cross point between the LOS and the ergodic layer. The plasma emissions from the six LOSs are transferred by the twelve optical fibers to the MH spectrometer. With this spectrometer, high resolution spectra of the Balmer-α, -β, and -γ lines of hydrogen atoms and the Fulcher-α band $Q1$ lines of $v' = v'' = 0$ and 2 transitions of hydrogen molecules are simultaneously observed, where v' and v'' are vibronic quantum numbers of the upper and lower states of the transition, respectively. Details of the MH spectrometer are described in [16–18].

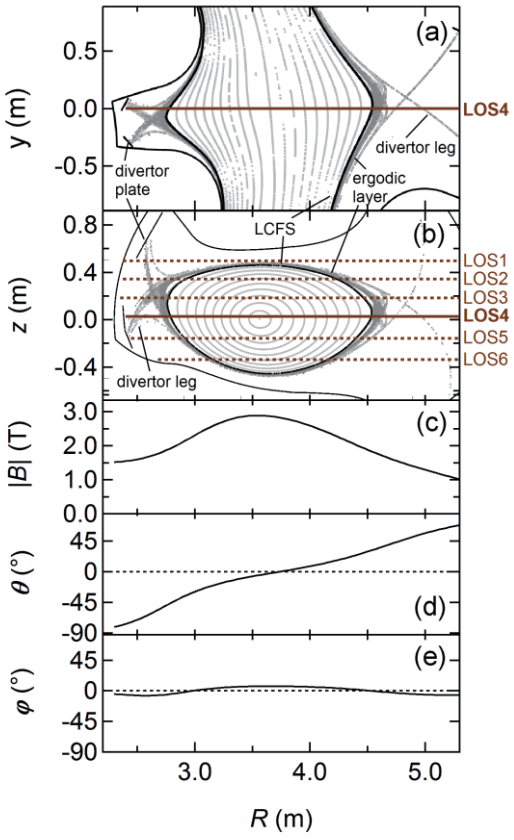

Fig. 1 (a) Toroidal and (b) poloidal cross sections of the LHD. The LCFS is indicated by black curves. The gray curves inside the LCFS show the magnetic flux surfaces. The gray regions outside the LCFS indicate the ergodic layer and the divertor legs. The LOSs are shown by horizontal lines. The toroidal cross section shown in (a) includes LOS4. The magnetic field distribution along the LOS4 is shown in (c), (d) and (e); (c) the magnetic field strength, $|B|$, (d) the pitch angle, θ, of the magnetic field from the horizontal plane of the LHD, and (e) the yaw angle, φ, between the projection of the magnetic field vector on the horizontal plane and the perpendicular direction to the LOS.

In this measurement, we increase the number of the optical fibers for light input and change the focus regions of the spectra on the photo-electric surface of the charge coupled device (CCD) of the MH spectrometer from that described in our previous paper [18]. For the purpose of explaining the focus regions, we show the two-dimensional image on the photo-electric surface of the CCD in Fig. 2 for emission from a low-pressure hydrogen discharge tube (Electro-Technic, SP200). The horizontal and vertical directions are parallel to the dispersion direction and the entrance slit, respectively. The spectra of the five emission lines are focused on the different regions of the photo-electric surface, which are indicated by colored squares in Fig. 2. Since we use twelve fiber inputs, twelve images align vertically in each region. The relation between the twelve images and the LOSs and their polarizations are indicated in the right of Fig. 2. The three atomic emissions and two molecular emissions are focused on the same

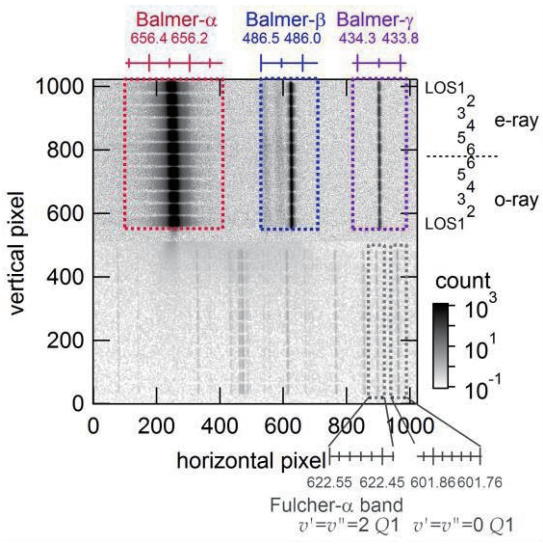

Fig. 2 A two-dimensional image on the photo-electric surface of the CCD obtained with a low-pressure hydrogen discharge tube at the twelve optical fibers input.

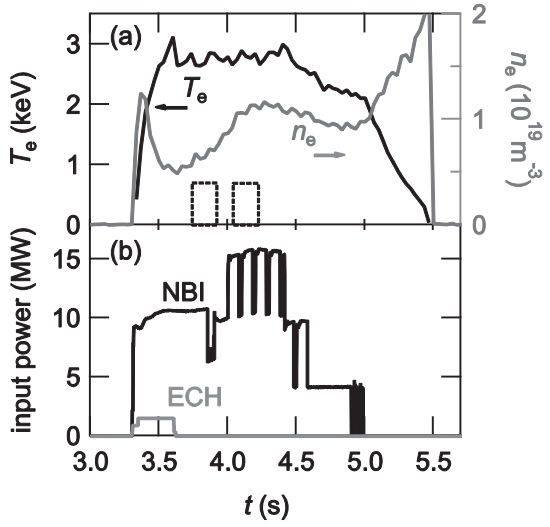

Fig. 3 Temporal development of (a) the electron temperature and density at the plasma center, and (b) the heating power. The exposure timings of the CCD are shown by dotted squares in (a).

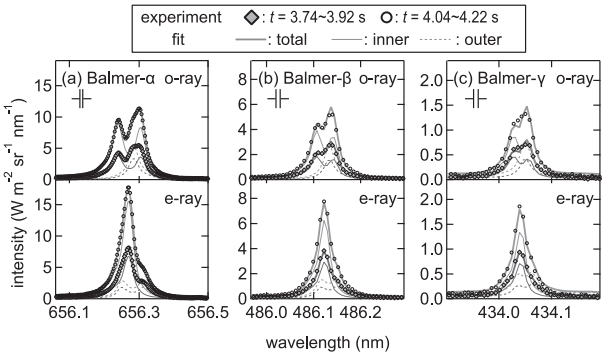

Fig. 4 Examples of the observed atomic spectra, (a) Balmer-α, (b) -β, and (c) -γ lines, for the LOS4. The o-ray and e-ray components of the spectra are shown in the upper and lower parts of the figures, respectively. The spectra taken in t = 3.74~3.92 s and 4.04~4.22 s are shown by diamonds and circles, respectively. The instrumental width for each wavelength region is shown by the interval of the vertical lines. The fitted results are shown by bold curves. The estimated spectra of the emissions from the inboard and outboard emission locations are shown by thin solid and dotted curves, respectively.

height of the CCD image plane as shown in Fig. 2. The corresponding wavelengths are indicated by the horizontal axes. While the wing part of the Balmer-α spectra overlaps the other ones, we confirmed such contaminations give negligible effect on the central regions of the spectra. The instrumental function for each wavelength region is similar to a single Gauss function. The instrumental widths for the Balmer-α, -β, -γ lines and the Fulcher-α band $Q1$ lines in the two vibronic transitions are 8, 9, 10, 8 and 7 pm, respectively, at a slit width of 20 μm. Thorium and Argon emission lines from a hollow cathode discharge tube (photoron, P858A) are used to calibrate the wavelength of the system. The sensitivity of the system is absolutely calibrated against a standard lamp with an integration sphere (Labsphere, USS-600C).

A hydrogen plasma is generated and sustained by the neutral beam injection (NBI) and electron cyclotron heating (ECH) in LHD (shot number: #96998). The time development of the electron temperature, T_e, and density, n_e, in the plasma center which are measured by the Thomson scattering system [19] is shown in Fig. 3 (a). The temporal change of the heating power is shown in Fig. 3 (b). The plasma is ignited at t = 3.3 s and the central temperature is sustained nearly stationary until 4.5 s. Two exposures of the CCD are made during the discharge in t = 3.74~3.92 s and t = 4.04~4.22 s. The exposure timings are shown by two dotted squares in Fig. 3 (a). In the second exposure time, the electron temperature is similar to that in the first exposure time, while the electron density is about twice of that in the first one.

3. Results and Discussion

Figure 4 shows the spectra of the Balmer-α, -β, and -γ lines observed for the LOS4. The upper parts of the figures show the o-ray components of the spectra while the lower ones show the e-ray components. The spectra taken in t = 3.74~3.92 s and 4.04~4.22 s are shown by diamonds and circles, respectively.

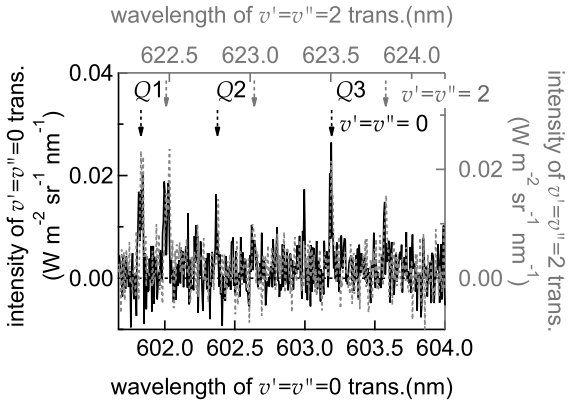

Fig. 5 Fulcher-α band Q branch spectra of the $v' = v'' = 0$ and 2 transitions observed for the LOS4 in t = 3.74~3.92 s. The o-ray and e-ray components are shown by solid and dotted lines, respectively. The central wavelengths of the $Q1$, $Q2$, and $Q3$ lines are indicated by vertical arrows. The intensities of the $v' = v'' = 0$ and 2 transition emissions are indicated in the left and right axes, respectively. The wavelengths of the two vibronic transitions are indicated in the top and bottom axes, respectively.

In Fig. 5, the Fulcher-α band $Q1$, $Q2$, and $Q3$ lines observed for the LOS4 in t = 3.74~3.92 s are shown. The o-ray and e-ray components are shown by solid and dotted lines, respectively. The central wavelengths of these Q branch spectra of $v' = v'' = 0$ and 2 transitions are indi-

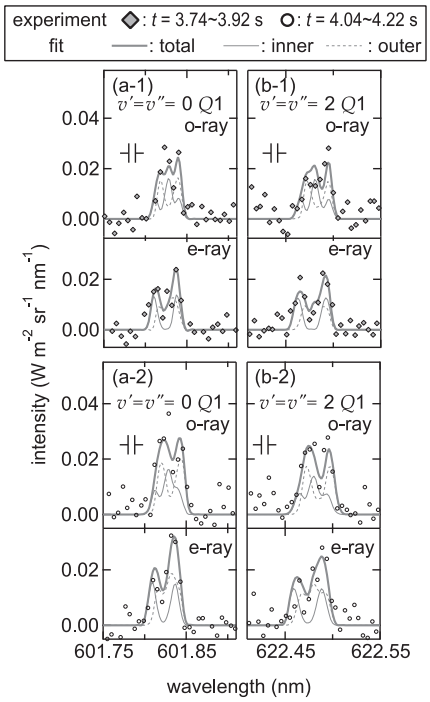

Fig. 6 Fulcher-α band $Q1$ line spectra of the (a-1, a-2) $v' = v''$ = 0 and (b-1, b-2) $v' = v'' = 2$. The spectra taken in t = 3.74~3.92 s and 4.04~4.22 s are shown in (a-1, b-1) and (a-2, b-2), respectively. The upper and lower parts of the figures show the o-ray and e-ray components of the spectra, respectively. The synthetic profiles are presented by thick curves. The estimated spectra of the emission from the inboard and outboard sides are shown by thin solid and dotted curves, respectively.

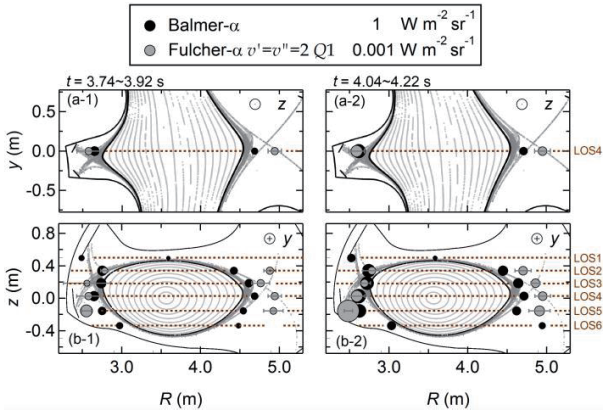

Fig. 7 Emission locations and intensities determined from the Zeeman profile analysis are shown by centers and areas of the circles, respectively (black circles for atoms, gray circles for molecules). (a-1, a-2) Toroidal cross sections of the LHD which include LOS4 (z = 0.026 m). (b-1, b-2) Poloidal cross sections. (a-1, b-1) and (a-2, b-2) show the results for the spectra taken in t = 3.74~3.92 s and 4.04~4.22 s, respectively. It is noted that the scales of the atomic and molecular emission intensities are different.

cated by vertical arrows in the figure. The spectra in the two vibronic transitions are focused on the same height of the CCD as shown in Fig. 2. We show the wavelengths for the $v' = v'' = 0$ and 2 transitions as the bottom and top axes, respectively. Since our system has small wavelength dependence of the sensitivities, the intensity of the spectra in the $v' = v'' = 0$ and 2 transition emissions are separately given in the left and right axes, respectively. In Fig. 6, detailed profiles of the two $Q1$ lines are shown. The spectra observed in t = 3.74~3.92 s and 4.04~4.22 s are plotted in (a-1, b-1) and (a-2, b-2), respectively.

The line splits and their polarization dependences due to the Zeeman effect can be seen in both the atomic and molecular spectra. We analyze the atomic and molecular line shapes with assuming the emission locations of the atoms and molecules are localized in two locations along each LOS, i.e. the inboard and outboard sides of the main plasma. From the magnetic field distribution along the LOS, the Zeeman profiles of the emission lines are reconstructed. The velocity distribution of atoms is assumed to be a linear combination of three Maxwell distributions [18], and the Doppler profile of the atomic lines is reconstructed from the distribution. The molecular velocity distribution is assumed to be a single Maxwell distribution. We fit the spectra of both the polarization components simultaneously by taking the Zeeman, Doppler, and instrumental profiles into account. From the fit, the emission locations and intensities are determined. The details of the analytical method are described in [9, 18].

The fit results are shown in Figs. 4 and 6 by bold curves. The observed spectra are well reconstructed by the analysis. In the figures, we also show the calculated spectra of the inboard and outboard sides by thin solid and dotted curves, respectively. The determined atomic emission locations and intensities for two exposure timings are plotted in Fig. 7 by centers and areas of the black circles, respectively. The determined molecular emission locations and intensities from the two $Q1$ lines are shown in Fig. 7 by gray circles. It is noted that since the intensities of the observed molecular lines for the LOS1 and the LOS6 are small and the signal to noise ratio is insufficient, no profile analyses are performed.

The determined atomic emission locations are just outside the LCFS for both the exposure timings. Nearly the same intensities are observed for the LOSs 2, 3, 4, and 5. On the other hand, the molecular emission locations are determined to be further positions from the plasma center than the atomic ones. Within the error bars, the molecular emission locations are on the divertor legs, where the electron temperature is smaller than the ergodic layer [20]. The tendency is consistent with the previous observation with two LOSs [18]. Larger molecular emission intensity is observed near the divertor plate. Since the ionization flux of the atoms and molecules are nearly proportional to the emission intensity of the Balmer-α line and the Fulcher-α band $Q1$ lines, respectively, in our density range [18, 21, 22], the central locations of the black and

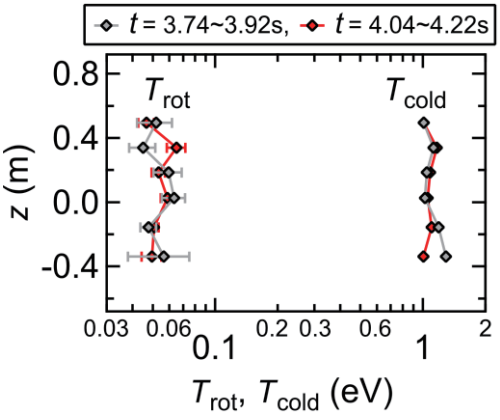

Fig. 8 Rotational temperatures of molecules, T_{rot}, for the six LOSs and for the two exposure timings. The cold temperatures of atoms estimated from the Balmer-α line shape analysis, T_{cold}, are also shown.

gray circles in Fig. 7 indicate the dominant ionization locations of the atoms and molecules, respectively.

The rotational temperature of the molecules is estimated from the line integrated intensities of the Fulcher-α band Q branch lines, an example of which is shown in Fig. 5. The analytical method is described in [13, 18]. The results are shown in Fig. 8. In the figure, the atomic temperature is also shown. The rotational temperature of the molecules is in the range of 0.04~0.07 eV, which are in the order of room temperature. The atomic temperature is about 1 eV, which may reflect the molecular dissociation energy. These tendencies are also consistent with our previous result [18]. The dependences of the temperatures on the LOSs or on the exposure timings are not clearly detected within the experimental accuracies.

4. Summary

We observe the linearly polarization-resolved spectral line shapes of the Balmer-α, -β, and -γ lines of hydrogen atoms and Fulcher-α band Q branches of molecules simultaneously for a hydrogen plasma generated in the LHD. We use six LOSs which cover the poloidal cross section of the LHD. From the analysis of the spectra including the line splits and their polarization dependences by the Zeeman effect, the emission locations, intensities and temperatures of the atoms and molecules are determined. The determined emission locations of the hydrogen atoms are just outside the LCFS while the molecular emission locations are close to the divertor legs. The molecular intensities are found to be large near the divertor plate in contrast to the relatively uniform intensity distribution of the atomic emissions. The determined atomic temperature is in the order of 1 eV, while the determined rotational temperature of molecules is 0.04~0.07 eV, both of which show no systematic dependence on the location within the experimental accuracy.

Acknowledgements

The authors are grateful to the LHD experimental group for their support. This work was supported by the National Institute for Fusion Science (Grant No. NIFS08KOAP020, NIFS10KLMP003).

[1] D.H. McNeill, J. Nucl. Mater. **162–164**, 476 (1989).
[2] U. Samm and TEXTOR-94 Team, Plasma Phys. Control. Fusion **41**, B57 (1999).
[3] S. Tamor, J. Comput. Phys. **40**, 104 (1981).
[4] M. Goto, K. Sawada, K. Fujii, M. Hasuo and S. Morita, Nucl. Fusion **51**, 023005 (2011).
[5] F. Wagner and U. Stroth, Plasma Phys. Control. Fusion **35**, 1321 (1993).
[6] N. Asakura, K. Shimizu, N. Hosogane, K. Itami, S. Tsuji and M. Shimada, Nucl. Fusion **35**, 381 (1995).
[7] J.L. Weaver, B.L. Welch, H.R. Griem, J. Terry, B. Lipschultz, C.S. Pitcher, S. Wolfe, D.A. Pappas and C. Boswell, Rev. Sci. Instrum. **71**, 1664 (2000).
[8] T. Shikama, S. Kado, H. Zushi, M. Sakamoto, A. Iwamae and S. Tanaka, Phys. Plasmas **11**, 4701 (2004).
[9] A. Iwamae, M. Hayakawa, M. Atake, M. Goto, S. Morita and T. Fujimoto, Phys. Plasmas **12**, 042501 (2005).
[10] A. Iwamae, A. Sakaue, N. Neshi, J. Yanagibayashi, M. Hasuo, M. Goto and S. Morita, J. Phys. B: At. Mol. Opt. Phys. **43**, 44019 (2010).
[11] A. Pospieszczyk, Ph. Mertens, A. Huber, D. Reiter, D. Rusbüldt, B. Schweer, E. Vietzke, P.T. Greenland and G. Sergienko, J. Nucl. Mater. **266**, 138 (1999).
[12] U. Fantz, B. Heger, D. Wünderlich and P. Pugno, J. Nucl. Mater. **313**, 743 (2003).
[13] B.P. Lavrov, A.A. Solovév and M.V. Tyutchev, J. Appl. Spec. **32**, 316 (1980).
[14] T. Shikama, S. Kado, H. Zushi, M. Sakamoto, A. Iwamae and S. Tanaka, Phys. Plasmas **11**, 4701 (2004).
[15] T. Shikama, S. Kado, H. Zushi and S. Tanaka, Phys. Plasmas **14**, 072509 (2007).
[16] K. Fujii, K. Mizushiri, T. Nishioka, T. Shikama, A. Iwamae, M. Goto, S. Morita, S. Kado, K. Sawada and M. Hasuo, Rev. Sci. Instrum. **81**, 033106 (2010).
[17] K. Fujii, T. Shikama, A. Iwamae, M. Goto, S. Morita and M. Hasuo, Plasma Fusion Res. **5**, S2079 (2010).
[18] K. Fujii, T. Shikama, M. Goto, S. Morita and M. Hasuo, Phys. Plasmas **20**, 012514 (2013).
[19] K. Narihara, I. Yamada, H. Hayashi and K. Yamauchi, Rev. Sci. Instrum. **72**, 1122 (2001).
[20] S. Masuzaki, T. Morisaki, N. Ohyabu, A. Komori, H. Suzuki, N. Noda, Y. Kubota, R. Sakamoto, K. Narihara, K. Kawahata, K. Tanaka, T. Tokuzawa, S. Morita, M. Goto, M. Osakabe, T. Watanabe, Y. Matsumoto, O. Motojima and LHD Experimental Group, Nucl. Fusion **42**, 750 (2002).
[21] K. Sawada, K. Eriguchi and T. Fujimoto, J. Appl. Phys. **73**, 8122 (1993).
[22] K. Sawada and T. Fujimoto, J. Appl. Phys. **78**, 2913 (1995).